The Rac1 exchange factor Dock5 is essential for bone resorption by osteoclasts.

Virginie Vives, Mélanie Laurin, Gaelle Cres, Pauline Larrousse, Zakia Morichaud, Danièle Noel, Jean-François Côté, Anne Blangy

The Rac1 exchange factor Dock5 is essential for bone resorption by osteoclasts.

Virginie Vives[1,2§], Mélanie Laurin[3], Gaelle Cres[1,2], Pauline Larrousse[1,2], Zakia Morichaud[4], Danièle Noel[5], Jean-François Côté[3] and Anne Blangy[1,2*]

[1] Montpellier Universities 1 and 2, CRBM, Montpellier, France

[2] CNRS, UMR5237, Montpellier, France.

[3] Institut de Recherches Cliniques de Montréal, Université de Montréal, Montréal, Québec H2W 1R7, Canada.

[4] CNRS, UMR5236, CPBS, Montpellier, France

[5] Inserm U844, Montpellier, France.

[§] Present address: IGMM, CNRS UMR5535, Montpellier, France.

* To whom correspondence should be addressed.

This work was supported by grants from the Fondation pour la Recherche Médicale (grant #DVO20081013473 to AB), from the Ligue contre le Cancer (grant#7FI9556JQSC, comité de l'Aude to AB), from the Arthritis Foundation Courtins (grant # OTP30713 to AB) and by the Canadian Institute of Health Research (CIHR) (to J-FC). VV was a recipient of a postdoctoral fellowship from the Association pour la Recherche sur le Cancer. J-FC holds a CIHR New Investigator award.

Running title: Osteoclasts need Dock5 to resorb bone.

Author's email addresses: virginie.vives@igmm.cnrs.fr, Melanie.Laurin@ircm.qc.ca, gaelle.cres@crbm.cnrs.fr, pauline.larrousse@crbm.cnrs.fr, zakia.morichaud@univ-montp1.fr, daniele.noel@inserm.fr, Jean-Francois.Cote@ircm.qc.ca

Corresponding author: Anne BLANGY, CNRS UMR 5237 CRBM, 1919 route de Mende, 34293 Montpellier Cedex 5. France, Tel: +33 467 613 422, Fax: +33 467 521 559, E-mail: anne.blangy@crbm.cnrs.fr

Abstract: Words: 203, Characters: 1256

Text: Words: 8,218 Characters: 45,357

7 figures: 3 color and 4 black and white figures.

All authors have no conflicts of interest.

Abstract.

Osteoporosis, which results from excessive bone resorption by osteoclasts, is the major cause of morbidity for elder people. Identification of clinically relevant regulators is needed to develop novel therapeutic strategies. Rho GTPases have essential functions in osteoclasts by regulating actin dynamics. This is of particular importance since actin cytoskeleton is essential to generate the sealing zone, an osteoclast-specific structure ultimately mediating bone resorption. Here, we report that the atypical Rac1 exchange factor Dock5 is necessary for osteoclast function both *in vitro* and *in vivo*. We uncovered that establishment of the sealing zone and consequently osteoclast resorbing activity *in vitro* require Dock5. Mechanistically, our results suggest that osteoclasts lacking Dock5 have impaired adhesion that can be explained by perturbed Rac1 and p130Cas activities. Consistent with these functional assays, we identified a novel small molecule inhibitor of Dock5 capable of hindering osteoclast resorbing activity. To investigate the *in vivo* relevance of these findings, we studied *Dock5*$^{-/-}$ mice and uncovered that they have increased trabecular bone mass, with normal osteoclast numbers, confirming that Dock5 is essential for bone resorption but not for osteoclast differentiation. Taken together, our findings characterize Dock5 as a regulator of osteoclast function and as a potential novel target to develop anti-osteoporotic treatments.

Key words: osteoclast, Rac1, Dock5, adhesion, inhibitor of bone resorption.

Introduction

Osteoporosis is now a major health problem worldwide, in particular due to general population aging. An important cause of osteoporosis is estrogen deficiency that results in excessive bone loss in postmenopausal women. Diverse conditions such as bone metastases, lack of physical activity, disability and inflammation also provoke osteoporosis. Although the mechanisms of these diseases are distinct, excessive activity of osteoclasts (OCs) is a common feature and hallmark of osteoporosis (1). OCs, the major bone resorbing cells, are derived from mononuclear precursors of the monocyte/macrophage lineage such as bone marrow macrophages (BMMs). In response to the cytokines RANKL (receptor activator of NF-kappaB ligand) and M-CSF, monocyte precursors differentiate into preOCs that ultimately fuse to form polykaryons with the capacity to resorb mineralized substrates such as bone (2). To initiate bone resorption, OCs polarize and undergo extensive morphological changes to form an actin ring, also known as the sealing zone (3). This OC specific adhesion structure is composed of densely packed podosomes (4). It surrounds the ruffled border, a differentiated region of the plasma membrane that secretes protons and proteases at the bone contact. This is the actual site of bone resorption (5). The activation of RANK receptor by RANKL elicits a complex transcriptional program during OC differentiation. The master OC transcription factor NFATc1 regulates many OC specific genes, in particular *ATP6v0d2* and *DC-STAMP*, involved in precursor fusion, and *Acp5*, *Ctsk*, *Src* and *ITGB3*, essential for bone resorption (6). At the bone surface, OCs cycle between resorptive and migratory phases. Assembly and disassembly of the sealing zone requires profound remodeling of the actin cytoskeleton (7), regulated by adhesion signaling molecules, including Src, Pyk2 and p130Cas, downstream of integrin αvß3 (8). As major cellular regulators of actin organization, Rho GTPase signaling pathways are also essential players in sealing zone assembly (9).

Rho GTPases cycle between inactive GDP-bound and active GTP-bound states. In their active form they bind to effector proteins and engage numerous signaling pathways. Efficient nucleotide replacement requires guanine nucleotide exchange factors (GEFs) that catalyze activation of Rho GTPases (10). These GEFs fall into two families: Dbl- and Dock-proteins. The Dock family of GEFs comprises 11 Dock1- (also known as Dock180-) related proteins in mammals (11,12). Docks are characterized by a unique DHR (or CZH)-2 domain, which catalyzes nucleotide exchange on Rac1 or Cdc42, and a DHR-1 domain that localizes the GEFs to phosphatidylinositol (3,4,5) phosphates enriched membranes. Dock1, Dock2 and Dock5 also contain an SH3 domain at the N-terminus and a poly proline domain at the C-terminus. Through these domains, Dock1 interacts with CrkII, Crk-L and ELMO proteins and promotes Rac1 activation for efficient actin remodeling, cell migration and adhesion, myoblast and macrophage fusion (12-15).

In a previous study, we found that RANKL activates the transcription of *Dock5* (16). In addition, Dock5 is among the membrane-associated proteins most significantly overexpressed in OCs as compared to macrophages (17). Here, we tested the idea that Dock5 could be a central player in the control of OC cytoskeleton dynamics and biological activity. We demonstrate that Dock5 is essential for formation of the sealing zone and consequently for bone resorption by OCs. In addition, interfering with Dock5 expression abrogated Rac1 activation and impaired OC integrin-mediated adhesion. Likewise, blocking Dock5-mediated activation of Rac1 using a novel small biochemical inhibitor strikingly decreased OC resorption activity. Importantly, mice bearing a genetic deletion of *Dock5* have increased trabecular bone mass, in agreement with a role of this GEF in bone resorption. Our findings therefore identify a novel molecular mechanism that regulates actin dynamics for sealing zone assembly in OCs. They further highlight Dock5 as a potential target for novel anti-osteoporotic treatments.

Materials and Methods

Mice.

Dock5$^{-/-}$ mice were previously described (14). Mice used were 4 to 8-week-old and were maintained at the animal facilities of the CNRS in Montpellier and of the IRCM in Montreal.

Histological analyses.

Femurs of 8-week old mice were fixed for one week in 10% formalin in PBS, embedded in Historesin (Leica), 7 µm sections stained with von Kossa and counterstained with von Gieson. Alternately, bones were decalcified in 10 % EDTA for 10 days, embedded in paraffin and 4.5 µm sections stained for TRAP activity and counterstained with a nuclear fast red. Measures were done in a standard zone in distal femur situated 250 µm from the growth plate excluding the primary spongiosa. Bone volume, total volume, OC numbers and bone perimeters were measured in the same region of interest on three adjacent slides, using Bioquant OSTEO II (Bioquant Image Analysis).

Production of OCs and osteoblasts.

BMMs were isolated from long bones of 4- to 8-week-old animals as described (16) and OCs obtained by culturing BMMs with RANKL (100 ng/ml) and M-CSF (10 ng/ml) (Peprotech) for 5 days. RAW264.7 cells were grown for 5 days with RANKL (50 ng/ml) to obtain OCs. For resorption, OCs were differentiated in multiwell chambers or on coverslips coated with calcium phosphate (Osteologic Biocoat, BD Bioscience) or in 96-well plates containing a bovine bone slice (IDS Nordic Bioscience). Mesenchymal stem cells (MSCs) were isolated from mouse bone marrow and grown as described (18). Osteogenesis was induced by culture at low density (3 X 10^4 cells in 6-well plates) for 21 days in osteogenic medium (DMEM supplemented with 10 % FBS, 2 mM glutamine and 0.05 mM ascorbic acid), supplemented

with 3mM NaH_2PO_4 for mineralization assays. Osteoblasts were characterized by alizarin red S staining of the secreted calcified extracellular matrix as previously described (18).

Microscopy, immunofluorescence and TRAP labeling.

OCs were fixed and stained for DNA, actin or vinculin or TRAP as described (16,19). Anti-vinculin antibody (Sigma) was revealed with Alexa Fluor 546-conjugated secondary antibody and actin stained with Alexa Fluor 360 or 488-conjugated phalloidin (Invitrogen). Preparations were mounted in Mowiol 40-88 (Sigma) and imaged with Zeiss Axioimager Z2 microscope with Coolsnap HQ2 camera for fluorescence and Coolsnap color Cf camera using Zeiss 40x PLAN-NEOFLUAR 1.3 oil DIC or Zeiss 20x PLAN-APOCHROMAT 0.8 or Zeiss 10X EC PLAN-NEOFLUAR 0.3. Images were acquired with MetaMorph 7.0 software (Molecular Devices). OC circularity was measured using ImageJ. OCs were counted manually in 96-well plates stained to reveal DNA and TRAP activity, except in figure 5F where they were counted automatically using a Cellomics Arrayscan VTI (Thermo Scientific). For scanning electron microscopy, OCs on bone slices were fixed in PBS containing 3% glutaraldehyde and post-fixed with 1% OsO_4 . After alcohol dehydration, OCs were dried in hexamethyldisilazane (Acros Organics, NJ, USA) for 2 min, coated with Gold-palladium and observed using a Hitachi S4000 scanning microscope at 10 kV.

Adhesion assays.

OCs differentiated in 96-well plates were incubated for 5 minutes in PBS supplemented or not with 0.25 mM EDTA. Wells were then rinsed with PBS, fixed, stained with 0.1% crystal violet, lysed and OD595 was measured as described (19). Each condition was performed in triplicate wells.

Plasmid DNAs.

Yeast expression vectors for Rac1 and Kinectin (20,21) and GFP-fused TrioN (22) were reported previously. The obtain full length Dock5 cDNA, BamH1-Kpn1 fragment of RIKEN clone E130320D18 (nucleotides 249 to 1,913 of Dock5 mRNA), was fused to the Kpn1-Not1 fragment of IMAGE clone 30106676 (nucleotides 1,914 to 6,461 of Dock5 mRNA). The whole was fused to GFP and was inserted into pMXs-puro (23), a gift from Dr Kitamura, Tokyo, Japan. Dock5 DHR2 domain (aminoacids E1119 to L1667) was cloned into pEGFP (Clontech) or myc tagged in pRs426Met (21). Dock5 and firefly luciferase shRNA expression vectors were described previously (16) as well as methods to produce and use retroviruses (16,19).

RT-PCR and primers.

RT-PCR analyses were performed as described (19). Amplification primers were 5'-GGCTGTGTTTACCGACGAGC-3' and 5'-CAAGCACGCGGACAATGTTG-3' for Calcitonin receptor, 5'-TCAGCTTCAGCATTCAGCCC-3' and 5'-ACTGCACGATTCCAGAGTCC-3' for Dock1 and 5'-AGCCTTGCATCTCCTGTGGC-3' and 5'-CATGCGTCCCTTGGATGCTG-3' for Dock2, 5'-GCG CTC TGT CTC TCT GAC CT-3' and 5'-GCC GGA GTC TGT TCA CTA CC-3' for Osteocalcin, 5'-AAT GCC CTG AAA CTC CAA AA-3' and 5'-AGG GGA ATT TGT CCA TCT CC-3' for Alkaline Phosphatase, 5'-TGT TCA GCT TTG TGG ACC TC-3' and 5'-TCA AGC ATA CCT CGG GTT TC-3' for Collagen I. Other primers were described: Gapdh, Dock5, Vav3, Src, TRAP, NFATc1, CtsK, Integrin ß3, DC-STAMP and ATP6v0d2 (16,19), OSCAR, CD44 (6) and ADAM8 (24).

Active Rac1 quantification.

GTP-bound Rac1 was pulled down from OC or 293T cell extracts using GST-fused PAK1 CRIB domain as described (22) and revealed by western blot with monoclonal anti-Rac1 antibodies (Transduction Laboratories) and anti-GFP polyclonal antibodies (Torrey Pines Biolabs). To activate Rac1, OCs at day 4 of differentiation were starved overnight in the presence of 2% serum, stimulated with 100 ng/ml M-CSF or lifted and replated onto vitronectin-coated plates for 30 minutes prior to lysis, and active Rac1 levels were measured G-LISA kit according to manufacturer's instructions (Cytoskeleton).

Immunoprecipitation, western blot and antibodies.

Antibodies for phosphorylated Erk-1/2 were from Cell Signaling and for total Erk1/2 from Santa Cruz. Antibodies for Crk, p130Cas and Pyk2 antibodies were from Transduction Laboratories. 4G10 phosphotyrosine specific antibodies were a gift from Dr Bettache, Montpellier, France. OC were lysed in lysis buffer (50 mM Tris pH 7.5, 120 mM NaCl, 1 mM EDTA, 6 mM EGTA, 1% NP-40, 20 mM NaF, 100 μM Na3VO4) and directly analyzed by western blot for total tyrosine phosphorylation analysis. For immunoprecipitation, precleared lysates were precipitated and analyzed by western blot with the appropriate antibodies. Immunocomplexes were visualized by the ECL Western Lightning Plus detection system (Perkin Elmer) with horseradish peroxidase-conjugated secondary antibodies (GE Healthcare) and quantified using ImageJ.

Resorption assays.

OCs in multiwell Osteologic Biocoat were fixed at day 7 of differentiation and calcium-phosphate was stained with von Kossa as described (19). The entire well surface was imaged using a Zeiss AxioimagerZ1 microscope. Well image was reconstituted and resorbed areas were measured using MetaMorph 7.0 software (Molecular Devices). For bone resorption

assays, OCs were derived from BMMs in 96-well plates containing bovine bone slices. At day 5 of differentiation, medium was changed with fresh medium. After 2 days, CTx concentrations were measured using Crosslap (IDS Nordic Bioscience). To reveal resorption pits, bone slices were incubated for 1 hour in peroxidase conjugated wheat-germ agglutinin (WGA) lectin (SIGMA) in PBS (20 µg/ml) followed by detection of peroxidase activity using SIGMAFAST according to manufacturer's instructions (SIGMA).

Yeast methods.

Screening for Dock5 inhibitors was performed in TAT7 yeast disrupted for erg6 essentially as described for the RhoGEF TrioN (20,21). Briefly, yeasts were grown in 96-well plates in histidine free and histidine complemented drop out medium supplemented with 1% DMSO and 100 µM of one of the 2,640 chemical compounds to be tested (ChemBridge™, San Diego, CA) (25). Growth curves were established by measuring OD600. Inhibitors were selected for their ability to inhibit selectively growth acceleration in histidine-free medium conferred by Dock5-DHR2 expression without affecting growth in histidine-supplemented medium.

Statistical analyses.

Statistical significances were determined using Mann-Whitney non-parametrical test.

RESULTS.

Dock5 is a Rac1 GEF associated with OC adhesion structures.

We previously identified *Dock5* as a RhoGEF gene strongly induced during RANKL-stimulated osteclastogenesis in RAW264.7 cells and BMMs (16) (Figure 1A). Purified antibodies directed against the C-terminal end of Dock5 (14) confirmed the great increase of Dock5 expression during osteoclastic differentiation of BMMs (Figure 1B) and RAW264.7 cells (Figure 1C). Previous *in vitro* observations suggested that Dock5 could activate the GTPase Rac1 (26). To confirm this on endogenous Rac1, we expressed in HEK-293T cells the DHR2 domain of mouse Dock5, lying between aminoacids M1132 and Y1661 and corresponding to the equivalent domain defined in Dock1 (11,27) (Figure 1D). Pull down assays, using the GTPase binding domain of the kinase PAK1 that selectively binds to active Rac1 and Cdc42, showed that Dock5 can activate endogenous Rac1 without affecting Cdc42 activity (Figure 1E, left panel). Expression of GFP fusion proteins was assessed by western blot (Figure 1E, right panel). GFP-tagged full length Dock5 expressed in RAW264.7 cell-derived OCs colocalizes with vinculin at the podosome belt (Figure 1F).

Dock5 is essential for OC function *in vitro*.

To investigate the role of Dock5 in OC biology, we downregulated Dock5 in RAW264.7 cells using shRNAs (16). Whereas complete silencing of Dock5 leads to massive detachment of cells around day 3 of differentiation (16), lower retroviral concentrations leading to moderate silencing of Dock5 protein (Figure S1A) allows efficient formation of TRAP positive mutlinucleated cells in response to RANKL (Figure S1B). Strikingly, these OCs seeded on calcium-phosphate-coated substrates do not form sealing zones (Figure S1C). Accordingly, they do not resorb the mineral substrate (Figure S1D). Consistently, OCs

derived from shDock5-expressing BMMs exhibit very few and small sealing zones (Figure S1E) and have reduced bone resorbing activity (Figure S1F). This suggests that Dock5 is involved in formation of the sealing zone and then, in bone resorption by OCs.

To further study the physiological role of Dock5 in OCs, we differentiated OCs from primary BMMs isolated from *Dock5*$^{+/+}$ and *Dock5*$^{-/-}$ mice (14). *Dock5*$^{-/-}$ BMMs differentiate into OCs defined as TRAP positive multinucleated cells (Figure 2A). But *Dock5*$^{-/-}$ OCs fail to assemble sealing zones when seeded on calcium-phosphate substrates (Figure 2B-C) and they do not resorb the calcium-phosphate mineral substrate (not shown). Electron micrograph of bone slices seeded with *Dock5*$^{-/-}$ OCs showed that they can adhere on bone, but they were never found associated with a resorption pit (Figure 2D). Staining with WGA lectin showed that bone slices seeded with *Dock5*$^{-/-}$ OCs have very few and small resorption pits (Figure 2E). Measurement of degradation products of C-terminal telopeptide of type I collagen (CTx) production in the culture medium indeed confirmed that *Dock5*$^{-/-}$ OCs are defective for bone resorption (Figure 2F).

These results characterize Dock5 as being essential for the formation of OC sealing zone and subsequent bone resorption.

Dock5 is necessary for Rac1 and p130Cas activation in OCs.

We next evaluated the importance of Dock5 for RANKL induced expression of osteoclastic marker genes exploiting *Dock5*$^{+/+}$ and *Dock5*$^{-/-}$ BMMs. Real-time Q-PCR did not reveal any defect in the expression of the 12 genes tested (Figure 3A). In particular, *ITGB3*, *Src* and *Vav3* that are involved in sealing zone formation are expressed at normal levels. We also noticed that Dock5 deficiency does not induce a compensatory overexpression of *Dock1* or *Dock2*, the closest *Dock5* paralogs (Figure 3B). Thus, suppression of Dock5 does not appear to prevent the establishment of the OC specific transcriptional program.

We then investigated how the absence of Dock5 may impact on the activation of Rac1 in OCs. M-CSF regulates OC cytoskeleton (28) and induces rapid activation of Rac1 leading to the phosphorylation of Erk1/2 (29,30). Integrin αvß3 stimulation by adhesion of OC onto vitronectin also activates Rac1 (29,31). In the absence of Dock5, we found that M-CSF induces normal Rac1 activation and Erk1/2 phosphorylation (Figure 3C-D) and adhesion stimulated activation of Rac1 is not affected (Figure 3E).

We then looked at the steady state level of Rac1 activity in adherent OCs under no stimulation. In this case, active Rac1 pull down assays showed a strong reduction in Rac1 activity in OCs derived from *Dock5*$^{-/-}$ BMMs or from RAW264.7 cells expressing Dock5 shRNAs (Figure 4A-B). *Dock5*$^{-/-}$ OCs exhibited very irregular shapes on plastic (Figure 4C) as confirmed by significantly reduced circularity (Figure 4D). Furthermore, *Dock5*$^{-/-}$ OCs are less resistant to detachment from the substrate upon EDTA treatment (Figure 4E). These results show that in the absence of Dock5, OCs have low levels of Rac1 activity associated with spreading and adhesion defects.

We next investigated candidate signaling molecules known to participate in the control of OC adhesion that could be linked to Dock5 and Rac1 signaling. The adaptor protein p130Cas is involved in actin organization in OCs (32-34). Dock1 is known to stimulate signaling from the CrkII-p130Cas complex by increasing p130Cas tyrosine phosphorylation (35), which in turn stimulates Rac1 activation by the GEF (36). Dock5 was shown to control epithelial cell spreading through its binding to CrkII (37). The overall tyrosine phosphorylation profile in adherent OCs was not modified in the absence of Dock5 (Figure 4F) but we found less p130Cas in phosphotyrosine specific immunoprecipitates of *Dock5*$^{-/-}$OC lysates (Figures 4G-H). Consistently, low levels of tyrosine phosphorylated p130Cas were found in *Dock5*$^{-/-}$OC extracts immunoprecipitated with p130Cas specific antibodies (Figure 4I-J). We also observed increased CrkII phosphorylation (Figure 4G-H), which is known to prevent binding

of CrkII to p130Cas (38). Conversely, phosphorylation of Pyk2, a partner of p130Cas in OCs involved in sealing zone formation (39,40), remained unchanged in the absence of Dock5 (Figure 4G-H).

Taken together, these results suggest that the absence of Dock5 in OCs leads to adhesion defects associated with defective activation of Rac1 and p130Cas.

A chemical inhibitor of Rac1 activation by Dock5 hinders OC bone resorbing activity.

To confirm the essential role of Rac1 activation by Dock5 in the resorption process, we sought for a chemical inhibitor of Dock5 exchange activity active in cell cultures. We therefore took advantage of a yeast-based assay that we have developed (20,22). We constructed a yeast strain where Rac1 activation by Dock5 DHR2 induces the expression of the *his3* reporter gene (Figure 5A), which leads to faster yeast growth in Histidine deprived medium (Figure 5B). We screened a library of 2,640 heterocyclic commercial chemical compounds as described previously (22) for molecules able to inhibit growth of Dock5 DHR2-expressing yeasts in Histidine deprived medium without affecting growth in Histidine complemented medium. Thus we identified C21: N-(3,5-dichlorophenyl)benzenesulfonamide (Figure 5C). C21 efficiently inhibits the activation of Rac1 by Dock5-DHR2 in HEK293T cells (Figure 5D) but has no effect on Rac1 activation by the GEF TrioN (22) (Figure 5E). OC survival assays showed that C21 provokes OC death at concentrations above 25 µM (Figure 5F). 25 µM C21 efficiently inhibits the resorption of calcium-phosphate matrices (not shown) and bone resorption, as assessed by measurement of CTx concentration in the culture medium of OCs (Figure 5G). In parallel, control OCs grown in the presence of DMSO or 25 µM C21 were stained for TRAP to ascertain C21 was not toxic (not shown). Dose response experiment confirmed that C21 efficiently inhibits bone resoption by OCs *in vitro* (Figure 5H).

These results show that a small chemical compound preventing Rac1 activation by Dock5 efficiently suppresses bone resorption by OCs *in vitro*.

Dock5 deficiency leads to increased trabecular bone mass in mouse.

We explored the tissue distribution of Dock5 in mice. Interestingly, we found no activation of *Dock5* transcription in the bone forming mature osteoblasts derived from MSCs (Figure 6A) while the expression of osteoblast differentiation marker genes showed a very strong increase (Figure 6B). Western blot analyses of protein extracts from a variety of mouse tissues showed that Dock5 is predominantly expressed in OCs, testis and placenta (Figure 6C). Although expressed in these latter tissues and in ovary (not shown), $Dock5^{-/-}$ mice breed normally (not shown), suggesting that Dock5 does not play an essential function in mouse reproduction. This shows that the expression of Dock5 is restricted to a very narrow set of tissues in mice, including bone degrading OCs and excluding bone forming osteoblasts.

Quantitative bone histomorphometry performed on histological slices revealed that trabecular bone volume to total volume ratio (BV/TV) is increased over 30% in $Dock5^{-/-}$ mice as compared to wild type animals: 19% ± 3.5 in $Dock5^{-/-}$ vs 14.3% ± 2.6 in $Dock5^{+/+}$ (Figure 6D-E). In parallel, we found that OC number per bone surface (OC/mm) is identical in both genotypes: 11.2 ± 3.4 OC/mm in $Dock5^{-/-}$ vs 12.5 ± 3.4 $Dock5^{+/+}$ (Figure 6F-G).

Together with our *in vitro* observations, these data are consistent with an essential role of Dock5 for bone resorption but not for differentiation of OCs.

Discussion

Increased bone resorption by OCs is associated with various physiological disorders and pathological situations including hormonal defects, inflammation and cancer. Our study provides evidence that inhibition of Dock5 could be a novel approach to regulate bone loss. Our data highlight the essential role of this atypical Rac1 exchange factor in bone resorption: in the absence of Dock5, OCs differentiate but are unable to resorb bone due to their inability to form a sealing zone. We show that inhibition of Rac1 activation by Dock5 using a small chemical compound can modulate bone resorption. Finally, we found that *Dock5*$^{-/-}$ mice have increased trabecular bone mass associated with normal number of OCs, showing that Dock5 is also essential for bone resorption *in vivo*.

Targeting small GTPase signaling pathways using nitrogen containing bisphosphonates (N-BPs) has long proven an efficient strategy to control bone resorption by OCs in a variety of pathological situations (41). N-BPs inhibit the C-terminal prenylation of small GTPases from the Ras, Rab and Rho families, inducing the accumulation of unprenylated small GTPases and provoking OC dysfunction and death (42). However, N-BPs target a wide range of small GTPases that control many signaling cascades, which may be a reason for the undesirable side effects arising from N-BPs-based treatments (43,44). Considerable effort is currently being made to develop novel antiresorptive agents by targeting processes more specific to OCs such as RANKL antibodies or Cathepsin K inhibitors (45). We found that Dock5 is predominantly expressed in OCs; in particular it is not expressed in osteoblasts, the bone forming cells. Furthermore, *Dock5*$^{-/-}$ mice do not present major phenotypic defects. This suggests that inhibiting Dock5 *in vivo* could reduce the activity of OCs without affecting bone formation and other physiological functions. Therefore, targeting Dock5 exchange activity could represent a valuable strategy for the development of novel anti-osteoporotic treatments.

We used several experimental approaches to investigate the function of Dock5 in OCs. While all consistently leading to the conclusion that Dock5 is essential for OC bone resorbing activity, the experimental systems used showed minor discrepancies. In particular, we did not observe any toxic effect of Dock5 shRNAs upon differentiating BMMs into OCs, contrarily to what we had observed in RAW264.7 cells (16). This may reflect high infection efficiency of RAW264.7 cells as compared to BMMs as we never obtained complete silencing of Dock5 in primary cells. The toxic effect observed in RAW264.7 cells is most likely due to off target effects resulting from high levels of shRNAs rather than complete silencing of Dock5 as differentiation of *Dock5*$^{-/-}$ BMMs into OCs does not result in cell death.

Rho GTPases are well-established regulators of the actin cytoskeleton, which is highly dynamic in OCs, in particular during the resorption process when podosomes reorganize into a sealing zone (4,7). We showed that among the many RhoGEF genes expressed in OCs, only *Dock5* and the RhoA GEF *Arhgef8* exhibit strong transcriptional activation during RANKL induced osteoclastogenesis (16). We confirm now that the expression of Dock5 protein is indeed much higher in OC as compared to BMMs. In line with our findings, Ha et al. reported a quantitative proteomic study (17) showing that after ATP6v0d2, which is critical for OC differentiation, Dock5 is the second most abundant membrane associated protein differentially expressed in OCs as compared to macrophages. Our results did not reveal a role for Dock5 during OC differentiation *per se*. *Dock5*$^{-/-}$ mice have a normal number of OCs and *Dock5*$^{-/-}$ BMMs efficiently differentiate *in vitro* into OCs that express all characteristic genes tested. Conversely, Rac1 was shown to be necessary for the expression of the OC markers TRAP and Cathepsin K (46). Therefore, it is likely that GEFs distinct from Dock5 are needed to activate Rac1 for the control of gene expression during OC differentiation. In particular, the exchange factor Vav3 is required for Rac1 activation and expression of late OC differentiation markers Calcitonin receptor, TRAP and Cathepsin K (31).

Normal induction of the differentiation program suggests that the defects we observed in *Dock5*$^{-/-}$ OCs result from signaling defects, although we cannot exclude that important but as yet unidentified genes require Dock5 for their transcriptional activation during differentiation. We found that the steady state activity of Rac1 is reduced in OCs lacking Dock5. Interestingly, we also found reduced phosphorylation of p130Cas in the absence of Dock5. In OCs, M-CSF was shown to induce the stable interaction of c-Fms with αvß3 integrin and p130Cas. This leads to the phosphorylation of p130Cas, which is involved in the formation of the sealing zone (32-34). Besides, Dock1 was shown to increase p130Cas phosphorylation and to positively regulate signaling from integrins to the p130Cas-Crk signaling complex (35), which favors Rac1 activation (47,48). Altogether, this suggests that Dock5 and p130Cas could be involved in a common signaling network to control the activation of Rac1 in OCs. Vav3 is also required for the formation of the sealing zone (31). Nevertheless, our findings suggest that the signaling pathways controlled by Dock5 and Vav3 during this process are distinct. Indeed, M-CSF and adhesion stimulated activation of Rac1 requires Vav3 (31) whereas we found that it is independent of Dock5. M-CSF and adhesion were shown to activate Vav3, which is then recruited with Rac1 at the plasma membrane of OCs (49). We found that Dock5 associates with OC podosome belt. A possible hypothesis would be that Dock5 and Vav3 regulate Rac1 activation at distinct locations in OCs and at different phases of bone resorption cycle (Figure 7). For efficient resorption, OCs alternate between spreading and resorption steps that involve disassembly and reformation of the sealing zone (7). After the end of a resorption step, activation of c-Fms by M-CSF and of integrins through adhesion would recruit and activate Vav3 at the plasma membrane, leading to rapid activation of Rac1 (28,49). This would allow OC spreading and actin remodeling necessary for the initiation of new sealing zone formation (Figure 7B). Then, stable interaction of c-Fms with αvß3 by promoting the assembly of a signaling scaffold involving the p130Cas-CrkII complex (34)

would sustain robust activation of Rac1 by Dock5 at the actin ring. This would allow the stabilization of the sealing zone necessary for efficient bone resorption (Figure 7C).

Dock5$^{-/-}$ mice are have increased trabecular bone volume with normal number of OCs. This is in line with our *in vitro* observations showing that Dock5 is essential for resorption but not for OC differentiation. Although the effect of Dock5 suppression is very drastic for OC activity *in vitro*, *Dock5*$^{-/-}$ animals do not show severe bone mass increase. The phenotype of *Dock5*$^{-/-}$ mice is consistent with the moderate osteopetrotic phenotype reported for mice with targeted deletion of Rac1 in OCs (46). The moderate phenotype of *Dock5*$^{-/-}$ mice may be due to adaptative physiological mechanisms that may compensate for the low resorbing activity of OCs *in vivo* but are not activated in the *in vitro* model of cultured OCs. In particular, we did not observe increased expression of *Vav3*, *Dock1* or *Dock2* in *Dock5*$^{-/-}$ OCs in culture. These or other Rac1 GEFs expressed in OCs (16) may complement partially Dock5 deficiency *in vivo*. In line with this hypothesis, we reported previously that Dock1 and Dock5 are partially redundant during muscle fiber formation (14). Consistent with the restricted distribution of Dock5, *Dock5*$^{-/-}$ mice do not present major phenotypic defects. In particular, they are fertile and breed normally while Dock5 is expressed in testis and placenta, suggesting that Dock5 may not play an essential role in these tissues. Therefore, inhibiting Dock5 to limit bone resorption is expected to have limited side effects on other physiological functions.

Using N-(3,5-dichlorophenyl)benzenesulfonamide (C21), we show that the inhibition of Dock5 exchange activity towards Rac1 can efficiently reduce OC bone resorbing activity. This confirms that the activation of Rac1 by Dock5 plays a major role in the resorption process. Furthermore, the identification of this model chemical compound suggests that Dock5 activity can be reduced using small cell permeant molecules and that developing inhibitors of Rac1 activation by Dock5 represents a novel approach to control bone resorption. C21 is not a general inhibitor of Rac activation as it does not affect TRIO

exchange activity. Nevertheless, we found that C21 also affects Dock1 and to a lesser extend Dock2 exchange activities (our unpublished observations). Although the efficiency seems lower on those two GEFs as compared to Dock5, this was expectable given the high level of similarity between the three DHR2 domains. Therefore, the toxic effect we observed on OCs when increasing the concentration of C21 may result from the inhibition of Dock1 and Dock2 or other exchange factors essential for the survival of OCs. We identified C21 using a screening methodology in yeast that we previously validated for the exchange factor Trio (20,22). It could be valuable to screen more chemical compound libraries with such an assay to provide a novel source of chemical frameworks from which to develop original antiresorptive molecules.

In summary, we have shown that Dock5 is essential for the formation of the sealing zone and then for bone resorption by OCs *in vitro* and *in vivo*. Moreover, we show that inhibition of Rac1 activation by Dock5 using a small chemical compound can efficiently reduce bone resorption by OCs. The expression of Dock5 is mainly restricted to OCs and it is absent from osteoblasts. Therefore, developing Dock5 inhibitors appears as a novel approach to generate original antiresorptive molecules that would target OC activity with reduced side effects.

References

1. Weitzmann MN, Pacifici R 2006 Estrogen deficiency and bone loss: an inflammatory tale. J Clin Invest 116(5):1186-94.
2. Teitelbaum SL, Ross FP 2003 Genetic regulation of osteoclast development and function. Nat Rev Genet 4(8):638-49.
3. Jurdic P, Saltel F, Chabadel A, Destaing O 2006 Podosome and sealing zone: specificity of the osteoclast model. Eur J Cell Biol 85(3-4):195-202.
4. Luxenburg C, Geblinger D, Klein E, Anderson K, Hanein D, Geiger B, Addadi L 2007 The architecture of the adhesive apparatus of cultured osteoclasts: from podosome formation to sealing zone assembly. PLoS ONE 2:e179.
5. Vaananen HK, Laitala-Leinonen T 2008 Osteoclast lineage and function. Arch Biochem Biophys 473(2):132-8.
6. Kim K, Lee SH, Ha Kim J, Choi Y, Kim N 2008 NFATc1 Induces Osteoclast Fusion Via Up-Regulation of Atp6v0d2 and the Dendritic Cell-Specific Transmembrane Protein (DC-STAMP). Mol Endocrinol 22(1):176-85.
7. Saltel F, Destaing O, Bard F, Eichert D, Jurdic P 2004 Apatite-mediated actin dynamics in resorbing osteoclasts. Mol Biol Cell 15(12):5231-41.
8. Nakamura I, Duong le T, Rodan SB, Rodan GA 2007 Involvement of alpha(v)beta3 integrins in osteoclast function. J Bone Miner Metab 25(6):337-44.
9. Ory S, Brazier H, Pawlak G, Blangy A 2008 Rho GTPases in osteoclasts: Orchestrators of podosome arrangement. Eur J Cell Biol 87(8-9):469-77.
10. Rossman KL, Der CJ, Sondek J 2005 GEF means go: turning on RHO GTPases with guanine nucleotide-exchange factors. Nat Rev Mol Cell Biol 6(2):167-80.

11. Cote JF, Vuori K 2002 Identification of an evolutionarily conserved superfamily of DOCK180-related proteins with guanine nucleotide exchange activity. J Cell Sci 115(Pt 24):4901-13.

12. Meller N, Merlot S, Guda C 2005 CZH proteins: a new family of Rho-GEFs. J Cell Sci 118(Pt 21):4937-46.

13. Cote JF, Vuori K 2007 GEF what? Dock180 and related proteins help Rac to polarize cells in new ways. Trends Cell Biol 17(8):383-93.

14. Laurin M, Fradet N, Blangy A, Hall A, Vuori K, Cote JF 2008 The atypical Rac activator Dock180 (Dock1) regulates myoblast fusion in vivo. Proc Natl Acad Sci U S A 105(40):15446-51.

15. Pajcini KV, Pomerantz JH, Alkan O, Doyonnas R, Blau HM 2008 Myoblasts and macrophages share molecular components that contribute to cell-cell fusion. J Cell Biol 180(5):1005-19.

16. Brazier H, Stephens S, Ory S, Fort P, Morrison N, Blangy A 2006 Expression profile of RhoGTPases and RhoGEFs during RANKL-stimulated osteoclastogenesis: identification of essential genes in osteoclasts. J Bone Miner Res 21(9):1387-98.

17. Ha BG, Hong JM, Park JY, Ha MH, Kim TH, Cho JY, Ryoo HM, Choi JY, Shin HI, Chun SY, Kim SY, Park EK 2008 Proteomic profile of osteoclast membrane proteins: identification of Na+/H+ exchanger domain containing 2 and its role in osteoclast fusion. Proteomics 8(13):2625-39.

18. Fritz V, Noel D, Bouquet C, Opolon P, Voide R, Apparailly F, Louis-Plence P, Bouffi C, Drissi H, Xie C, Perricaudet M, Muller R, Schwarz E, Jorgensen C 2008 Antitumoral activity and osteogenic potential of mesenchymal stem cells expressing the urokinase-type plasminogen antagonist amino-terminal fragment in a murine model of osteolytic tumor. Stem Cells 26(11):2981-90.

19. Brazier H, Pawlak G, Vives V, Blangy A 2009 The Rho GTPase Wrch1 regulates osteoclast precursor adhesion and migration. Int J Biochem Cell Biol 41(6):1391-401.

20. Blangy A, Bouquier N, Gauthier-Rouviere C, Schmidt S, Debant A, Leonetti JP, Fort P 2006 Identification of TRIO-GEFD1 chemical inhibitors using the yeast exchange assay. Biol Cell 98(9):511-22.

21. De Toledo M, Colombo K, Nagase T, Ohara O, Fort P, Blangy A 2000 The yeast exchange assay, a new complementary method to screen for Dbl- like protein specificity: identification of a novel RhoA exchange factor. FEBS Lett 480(2-3):287-92.

22. Bouquier N, Vignal E, Charrasse S, Weill M, Schmidt S, Leonetti JP, Blangy A, Fort P 2009 A cell active chemical GEF inhibitor selectively targets the Trio/RhoG/Rac1 signaling pathway. Chem Biol 16(6):657-66.

23. Kitamura T, Koshino Y, Shibata F, Oki T, Nakajima H, Nosaka T, Kumagai H 2003 Retrovirus-mediated gene transfer and expression cloning: powerful tools in functional genomics. Exp Hematol 31(11):1007-14.

24. Choi SJ, Han JH, Roodman GD 2001 ADAM8: a novel osteoclast stimulating factor. J Bone Miner Res 16(5):814-22.

25. Andre E, Bastide L, Villain-Guillot P, Latouche J, Rouby J, Leonetti JP 2004 A multiwell assay to isolate compounds inhibiting the assembly of the prokaryotic RNA polymerase. Assay Drug Dev Technol 2(6):629-35.

26. Cote JF, Vuori K 2006 In vitro guanine nucleotide exchange activity of DHR-2/DOCKER/CZH2 domains. Methods Enzymol 406:41-57.

27. Yang J, Zhang Z, Roe SM, Marshall CJ, Barford D 2009 Activation of Rho GTPases by DOCK exchange factors is mediated by a nucleotide sensor. Science 325(5946):1398-402.

28. Faccio R, Takeshita S, Colaianni G, Chappel J, Zallone A, Teitelbaum SL, Ross FP 2007 M-CSF regulates the cytoskeleton via recruitment of a multimeric signaling complex to c-Fms Tyr-559/697/721. J Biol Chem 282(26):18991-9.

29. Faccio R, Novack DV, Zallone A, Ross FP, Teitelbaum SL 2003 Dynamic changes in the osteoclast cytoskeleton in response to growth factors and cell attachment are controlled by beta3 integrin. J Cell Biol 162(3):499-509.

30. Yan J, Chen S, Zhang Y, Li X, Li Y, Wu X, Yuan J, Robling AG, Kapur R, Chan RJ, Yang FC 2008 Rac1 mediates the osteoclast gains-in-function induced by haploinsufficiency of Nf1. Hum Mol Genet 17(7):936-48.

31. Faccio R, Teitelbaum SL, Fujikawa K, Chappel J, Zallone A, Tybulewicz VL, Ross FP, Swat W 2005 Vav3 regulates osteoclast function and bone mass. Nat Med 11(3):284-90.

32. Elsegood CL, Zhuo Y, Wesolowski GA, Hamilton JA, Rodan GA, Duong le T 2006 M-CSF induces the stable interaction of cFms with alphaVbeta3 integrin in osteoclasts. Int J Biochem Cell Biol 38(9):1518-29.

33. Nakamura I, Jimi E, Duong LT, Sasaki T, Takahashi N, Rodan GA, Suda T 1998 Tyrosine phosphorylation of p130Cas is involved in actin organization in osteoclasts. J Biol Chem 273(18):11144-9.

34. Nakamura I, Rodan GA, Duong le T 2003 Distinct roles of p130Cas and c-Cbl in adhesion-induced or macrophage colony-stimulating factor-mediated signaling pathways in prefusion osteoclasts. Endocrinology 144(11):4739-41.

35. Kiyokawa E, Hashimoto Y, Kurata T, Sugimura H, Matsuda M 1998 Evidence that DOCK180 up-regulates signals from the CrkII-p130(Cas) complex. J Biol Chem 273(38):24479-84.

36. Kiyokawa E, Hashimoto Y, Kobayashi S, Sugimura H, Kurata T, Matsuda M 1998 Activation of Rac1 by a Crk SH3-binding protein, DOCK180. Genes Dev 12(21):3331-6.

37. Sanders MA, Ampasala D, Basson MD 2009 DOCK5 and DOCK1 regulate Caco-2 intestinal epithelial cell spreading and migration on collagen IV. J Biol Chem 284(1):27-35.

38. Kobashigawa Y, Sakai M, Naito M, Yokochi M, Kumeta H, Makino Y, Ogura K, Tanaka S, Inagaki F 2007 Structural basis for the transforming activity of human cancer-related signaling adaptor protein CRK. Nat Struct Mol Biol 14(6):503-10.

39. Gil-Henn H, Destaing O, Sims NA, Aoki K, Alles N, Neff L, Sanjay A, Bruzzaniti A, De Camilli P, Baron R, Schlessinger J 2007 Defective microtubule-dependent podosome organization in osteoclasts leads to increased bone density in Pyk2(-/-) mice. J Cell Biol 178(6):1053-64.

40. Lakkakorpi PT, Nakamura I, Nagy RM, Parsons JT, Rodan GA, Duong LT 1999 Stable association of PYK2 and p130(Cas) in osteoclasts and their co-localization in the sealing zone. J Biol Chem 274(8):4900-7.

41. Rodan GA, Martin TJ 2000 Therapeutic approaches to bone diseases. Science 289(5484):1508-14.

42. Russell RG, Watts NB, Ebetino FH, Rogers MJ 2008 Mechanisms of action of bisphosphonates: similarities and differences and their potential influence on clinical efficacy. Osteoporos Int.

43. Kennel KA, Drake MT 2009 Adverse effects of bisphosphonates: implications for osteoporosis management. Mayo Clin Proc 84(7):632-7; quiz 638.

44. Recker RR, Lewiecki EM, Miller PD, Reiffel J 2009 Safety of bisphosphonates in the treatment of osteoporosis. Am J Med 122(2 Suppl):S22-32.

45. Deal C 2009 Future therapeutic targets in osteoporosis. Curr Opin Rheumatol 21(4):380-5.

46. Wang Y, Lebowitz D, Sun C, Thang H, Grynpas MD, Glogauer M 2008 Identifying the relative contributions of rac1 and rac2 to osteoclastogenesis. J Bone Miner Res 23(2):260-70.

47. Sharma A, Mayer BJ 2008 Phosphorylation of p130Cas initiates Rac activation and membrane ruffling. BMC Cell Biol 9:50.

48. Smith HW, Marra P, Marshall CJ 2008 uPAR promotes formation of the p130Cas-Crk complex to activate Rac through DOCK180. J Cell Biol 182(4):777-90.

49. Sakai H, Chen Y, Itokawa T, Yu KP, Zhu ML, Insogna K 2006 Activated c-Fms recruits Vav and Rac during CSF-1-induced cytoskeletal remodeling and spreading in osteoclasts. Bone 39(6):1290-301.

Acknowledgements

We want to thank Romain Dacquin for technical advice to perform bone histology and Jean-Paul Leonetti for sharing his chemical compound library. This work was supported by grants from the Fondation pour la Recherche Médicale (grant #DVO20081013473 to AB), from the Ligue contre le Cancer (grant#7FI9556JQSC, comité de l'Aude to AB), from the Arthritis Foundation Courtins (grant # OTP30713 to AB) and by the Canadian Institute of Health Research (CIHR) (to J-FC). VV was a recipient of a postdoctoral fellowship from the Association pour la Recherche sur le Cancer. J-FC holds a CIHR New Investigator award. The authors have no conflicting financial interests.

Figure Legends

Figure 1: Dock5 is a Rac1 exchange factor expressed in OCs.

(A) Total RNA of BMMs induced for differentiation in the presence of RANKL and M-CSF was extracted at days 0, 1, 2, 3 and 4 and levels of Dock5 and Cathepsin K (CtsK) mRNAs relative to Gapdh mRNA were determined by RT-PCR. (B-C) Total cell extracts were prepared from (B) BMMs treated as (A) or (C) from RAW264.7 cells grown for the indicated time in the presence of RANKL. Dock5 protein expression was visualized by western blot. (D) Alignment of the aminoacid sequences of the DHR2 exchange domains of mouse Dock5 and Dock1(11). Black background highlights residues conserved between the two sequences. (E) Total cell extracts were prepared from 293T cells expressing GFP-fused Dock5-DHR2 or GFP and submitted to GTP-trapping using the GST-fused CRIB domain of PAK1. Pulled-down and total Rac1 and Cdc42 (left panel) and GFP-fusion proteins in total cell extracts (right panel) were revealed by western blot. (F) Localization of GFP-tagged full length Dock5 (green) expressed in RAW264.7-derived OCs was visualized by fluorescence microscopy after staining for vinculin (red) and F-actin (blue) to reveal the podosome belt. Last panel is an enlarged view of boxed areas where yellow color reveals colocalization of Dock5 and vinculin. Scale bar 20 μm.

Figure 2: Dock5 is necessary for bone resorption by OCs derived from BMMs.

(A) OCs were differentiated from *Dock5*$^{+/+}$ (*+/+*) and *Dock5*$^{-/-}$ (*-/-*) BMMs and stained for TRAP activity. Scale bars 200 μm. (B) OCs were differentiated on Osteologic Biocoat from Dock5$^{+/+}$ and *Dock5*$^{-/-}$ BMMs and stained for actin to reveal the sealing zones (arrows). Insets show enlarged boxed areas. Scale bars 100 μm. (C) Proportion of OCs obtained as in (B) with a sealing zone. Graph shows average and SD of three independent OC preparations counting

over 300 cells. a: p<0.001, Mann-Whitney test. (D) Scanning electron micrographs showing OCs differentiated on bone slices. Arrows point at resorption pits. (E) Bone slices from (D) were stained with WGA lectin to reveal resorption pits (Arrows). (F) CTx concentrations measured in the culture medium of OCs grown on bone slices as in (D-E). Graph shows average and SD CTx concentration per OC relative to *Dock5*$^{+/+}$ control OC from three independent experiments performed in triplicate. a: p<0.001, Mann-Whitney test .

Figure 3: Dock5 is dispensable for the expression of OC characteristic genes and for Rac1 activation in response to M-CSF and adhesion.

(A-B) Total RNAs were prepared from *Dock5*$^{+/+}$ (*+/+*) and *Dock5*$^{-/-}$ (*-/-*) BMMs grown for 5 days in the presence of M-CSF (black bars) or of RANKL and M-CSF (white bars). mRNAs levels of OC characteristic genes (A) and from *Dock1* and *Dock2* (B) relative to Gapdh were determined by RT-PCR. (C) Rac1 activity was measured by G-LISA in *Dock5*$^{+/+}$ and *Dock5*$^{-/-}$ OCs at day 4 of differentiation stimulated with 100 ng/ml M-CSF for the indicated amount of time. (D) The levels of total and phosphorylated ERK1/2 were determined by western blot in *Dock5*$^{+/+}$ and *Dock5*$^{-/-}$ OCs stimulated with M-CSF as in (C). (E) Rac1 activity was measured by G-LISA in *Dock5*$^{+/+}$ and *Dock5*$^{-/-}$ OCs at day 4 of differentiation lifted and left in suspension (s) or replated onto vitronectin coated plates for 30 minutes (a). (C) and (E) show average active Rac1 and SD of duplicate measures in one experiment representative of two independent OC preparations.

Figure 4: Dock5 deficient OCs have less active Rac1 and adhesion defects and reduced p130Cas phosphorylation.

(A) Western blot showing total and GTP-bound Rac1 in extracts of *Dock5*$^{-/-}$ and *Dock5*$^{+/+}$ OCs. (B) Western blots showing total and GTP-bound Rac1 (left panel) and Dock5 and

Gapdh (right panel) in extracts of RAW264.7-derived OCs expressing Dock5 (shDock5) or control (shLuc) shRNAs. Figures in (A) and (B) show average and SD active Rac1 levels in Dock5 deficient OCs relative to controls in two independent experiments, western blots show one experiment. (C) *Dock5*$^{+/+}$ and *Dock5*$^{-/-}$ OCs were stained for TRAP to reveal global cell shape. Scale bars 200 µm. (D) OC average and SD circularity (4πxarea/perimeter^2) from four independent OC preparations measuring at least 60 OCs from 4 independent microscope fields in each experiment. a: $p<0.001$, Mann-Whitney test. (E) OCs remaining bound after 5 minutes incubation with the indicated concentration of EDTA, determined by crystal violet staining. Graph represents average and SD of two independent experiments performed in triplicates. b: $p<0.01$, n.s.: non significant change, Mann-Whitney test. (F) Western blot revealing global tyrosine phosphorylation with 4G10 antibody in OC lysates. (G) Western blots showing p130Cas (Cas), Pyk2 and Crk in control (-) or 4G10 immunoprecipitates (IP) and in total lysates (TCL). (H) Average and SD levels of p130Cas (Cas), Pyk2 and Crk phosphorylation in OCs from two independent experiments, one is shown in (G). a: $p<0.001$, n.s.: non significant change, Mann-Whitney test. (I) Western blot showing phosphorylated p130Cas (PCas) revealed by 4G10 and total p130Cas (Cas) in p130Cas immunoprecipitates of OC lysates. (J) Quantification of phosphorylated versus total p130Cas in the experiment shown in (I).

Figure 5: Inhibition of bone resorption by an inhibitor of Rac1 activation by Dock5.

(A) Principle of the yeast exchange assay used to identify inhibitors of Dock5 exchange activity. Wild type Rac1 is fused to LexA DNA binding domain (LexA) and its effector Kinectin (Kin) to GAL4 activation domain (GAD). Expression of Dock5-DHR2 activates Rac1, which binds to kinectin, leading to the expression of his3 and then yeast auxotrophy for histidine. Inhibitors of Dock5-DHR2 revert Rac1 activation. (B) Growth curves of yeasts

expressing Rac1 and Kinectin with (open triangles) and without (dots) Dock5-DHR2, in medium complemented (plain lines) or not (dotted lines) with histidine. (C) Structure of N-(3,5-dichlorophenyl)benzenesulfonamide (C21). (D) Western blots showing total and GTP-bound Rac1 (upper panels) and GFP and GFP-fused Dock5-DHR2 in extracts of 293T cells treated for 1 hour with the indicated concentrations of C21 in the presence of 1% DMSO. (E) Western blots showing total and GTP-bound Rac1 (upper panels) and GFP and GFP-fused TrioN in extracts of 293T cells treated as in (D). (F) Number of OCs (OC) after a 24-hour incubation with the indicated concentrations of C21, expressed as a % of DMSO control (0 µM C21). Graph shows average and SD of two to three independent experiments performed in triplicates. (G) CTx concentration in the medium of OCs on bone in the absence (0) or presence of 25 µM C21. Graph shows average and SD of three experiments performed in duplicates with independent OC preparations. a: $p<0.001$, Mann-Whitney test. (H) CTx production per OC in the presence of the indicated concentration of C21. Graph shows average and SD CTx concentration per OC in one experiment performed in triplicates.

Figure 6: Suppression of Dock5 leads to reduced trabecular bone mass in mice.

(A) Levels of Dock5 mRNA relative to Gapdh mRNA determined by RT-PCR in BMMs grown with M-CSF (ND) or differentiated into OCs for 5 days (D5) and in proliferating MSCs and MSC-derived osteoblasts (OB) (B) mRNA levels of the indicated osteoblast differentiation marker genes relative to Gapdh in proliferating MSCs and osteoblasts from (A) and mineralization activity of the osteoblasts revealed by Alizarin Red S staining. (C) Total proteins extracted from BMMs grown with M-CSF (ND) or for 3 and 5 days with M-CSF and RANKL and from various mouse tissues (Ey: Eye, Sp: Spleen, St: Stomach, Te: Testis, Pl: Placenta, Lu: Lung, Br: Brain, He: Heart, Li: Liver, Ki: Kidney; Mu: Muscle) were analyzed by western blot with antibodies against Dock5 and against tubulin for normalization. (D) Percent bone volume/total volume (BV/TV) in distal femur of 7-week-old mice (n=6). a:

$p<0.001$, Mann-Whitney test. (E) Histological section showing distal femur of 7-week-old mice stained with von Kossa to reveal mineralized tissue. (F) OC number per bone perimeter (OC/mm) in distal femur of 7-week-old mice (n=6). (G) Histological sections from distal femur of 7-week-old mice stained for TRAP activity to visualize OCs and counterstained with hematoxylin to visualize bone trabeculae.

Figure 7: Model for the respective functions of Dock5 and Vav3 during OC resorption cycle. OCs alternate between resorption and spreading phases (7). (A) At the end of a resorption phase, the sealing zone disassembles (dotted thick black line) around the newly formed resorption pit (dashed area). (B) Under the stimulation of M-CSF, Vav3 gets activated and in turn activates Rac1 downstream of c-Fms, allowing the OC to spread away from its previous resorption pits (arrows) and the initiation of a new sealing zone (thick black circle). (C) Then the stable interaction of c-Fms with αvß3 promotes the assembly of the p130Cas-CrkII signaling scaffold to sustain robust activation of Rac1 by Dock5, allowing the enlargement and stabilization of the sealing zone (arrows) for an efficient new bone resorption step (D).

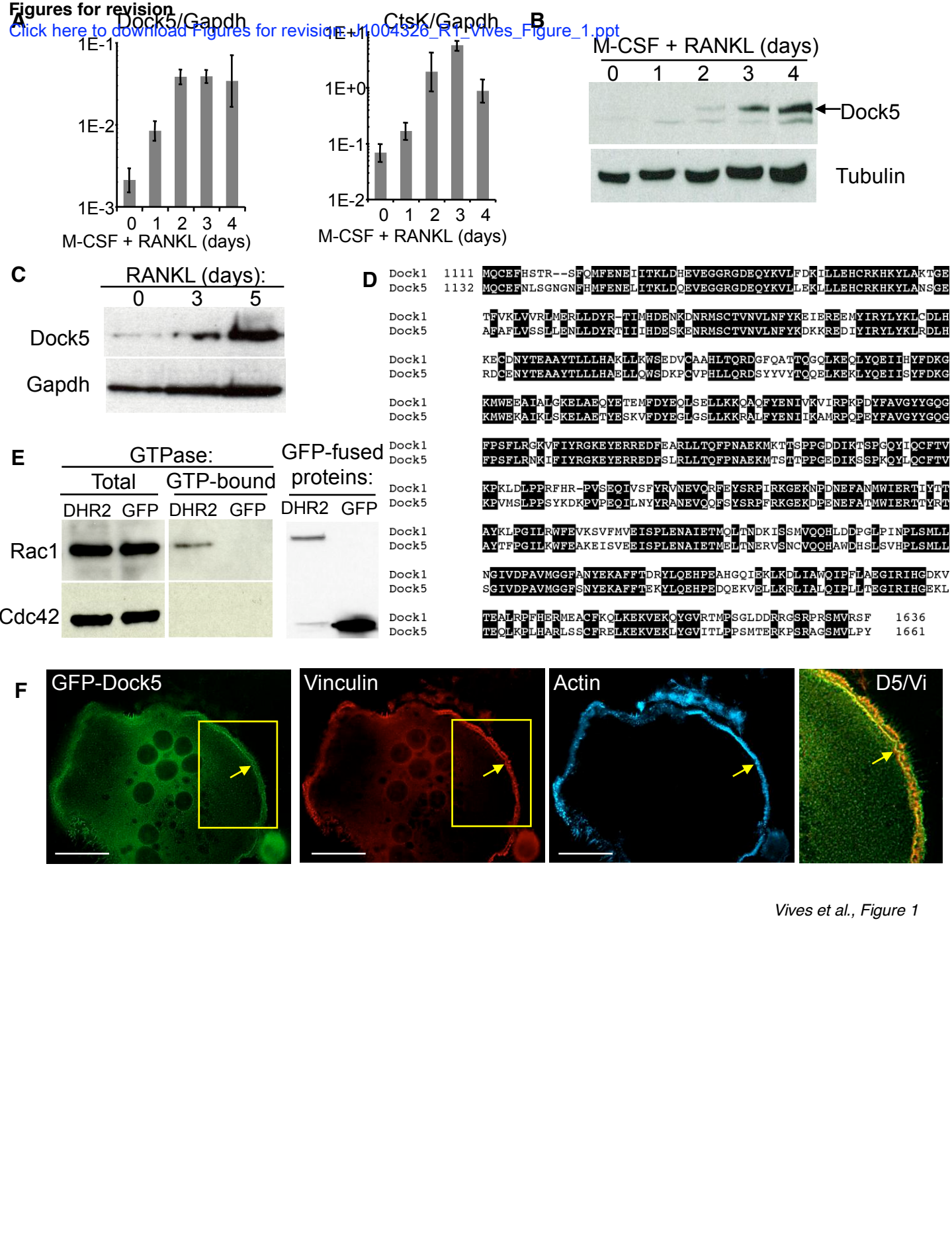

Vives et al., Figure 1

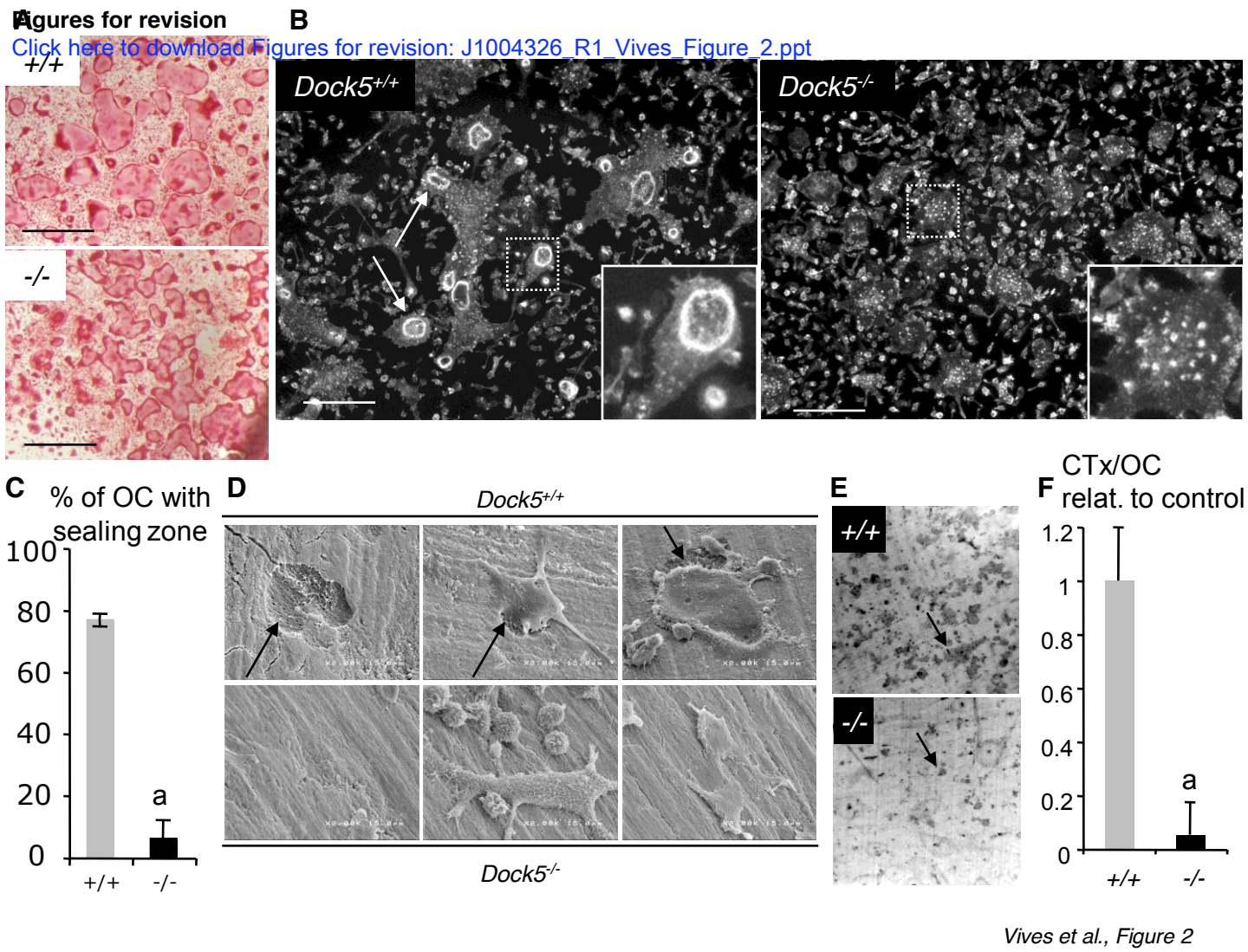

Vives et al., Figure 2

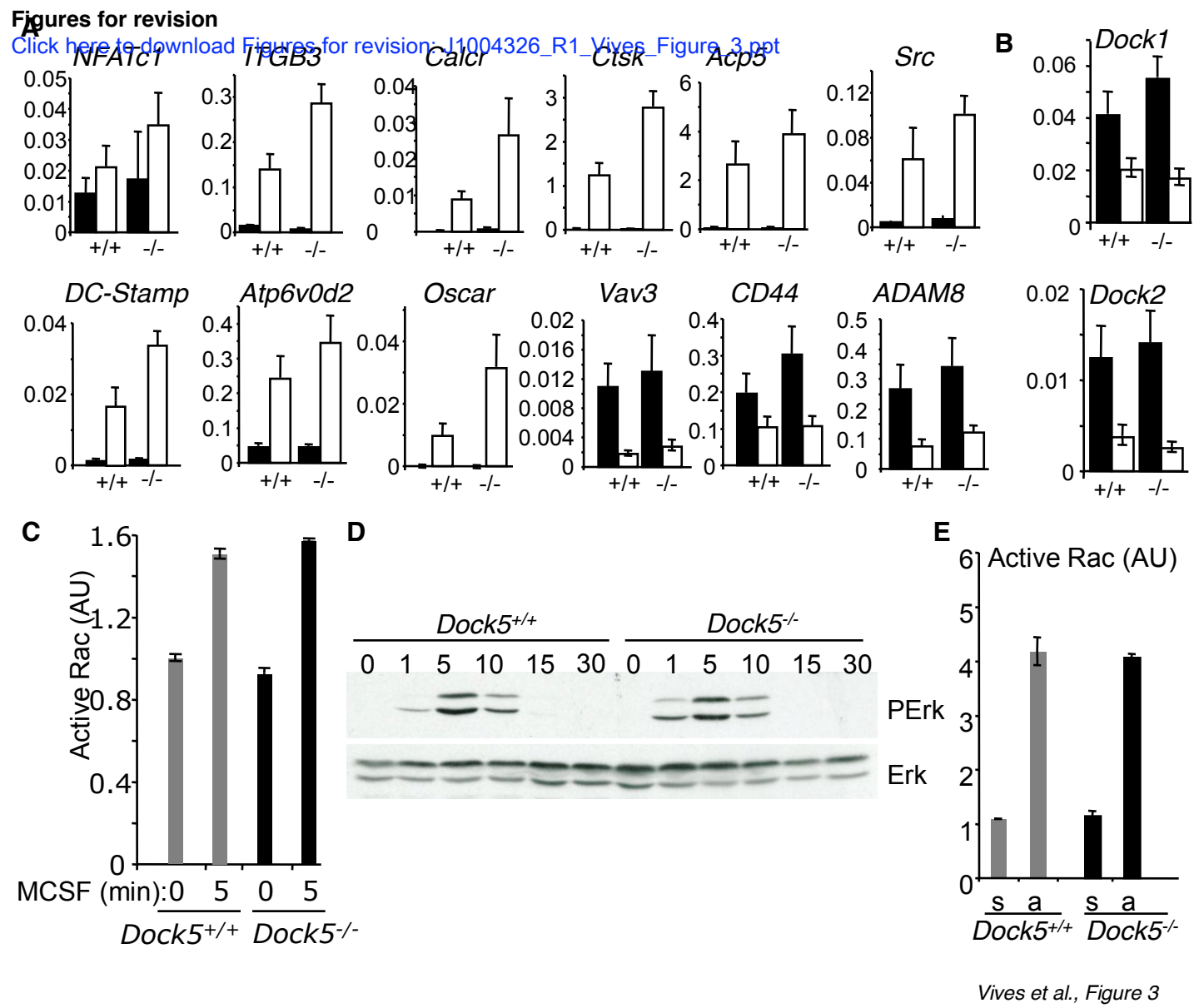

Vives et al., Figure 3

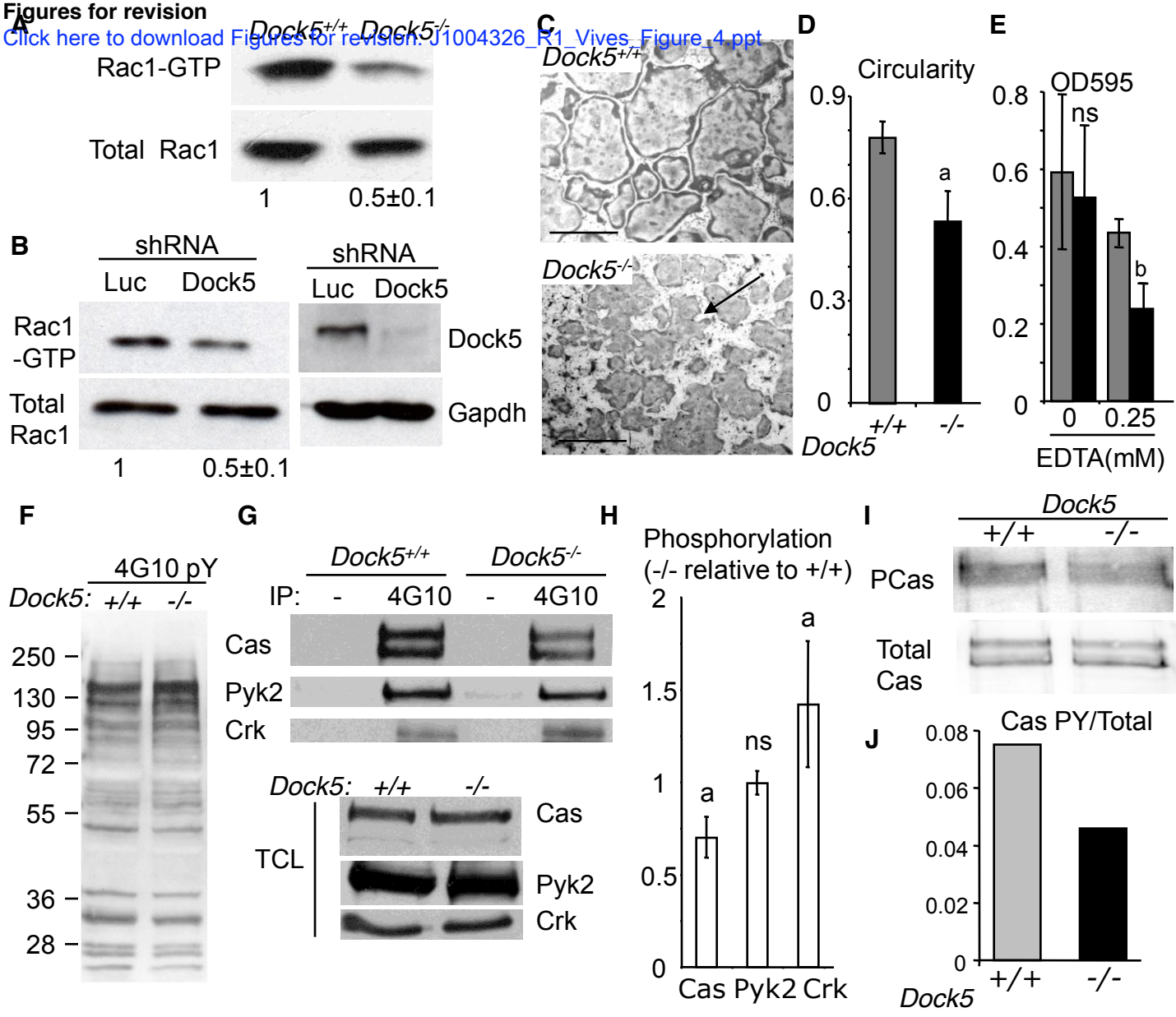

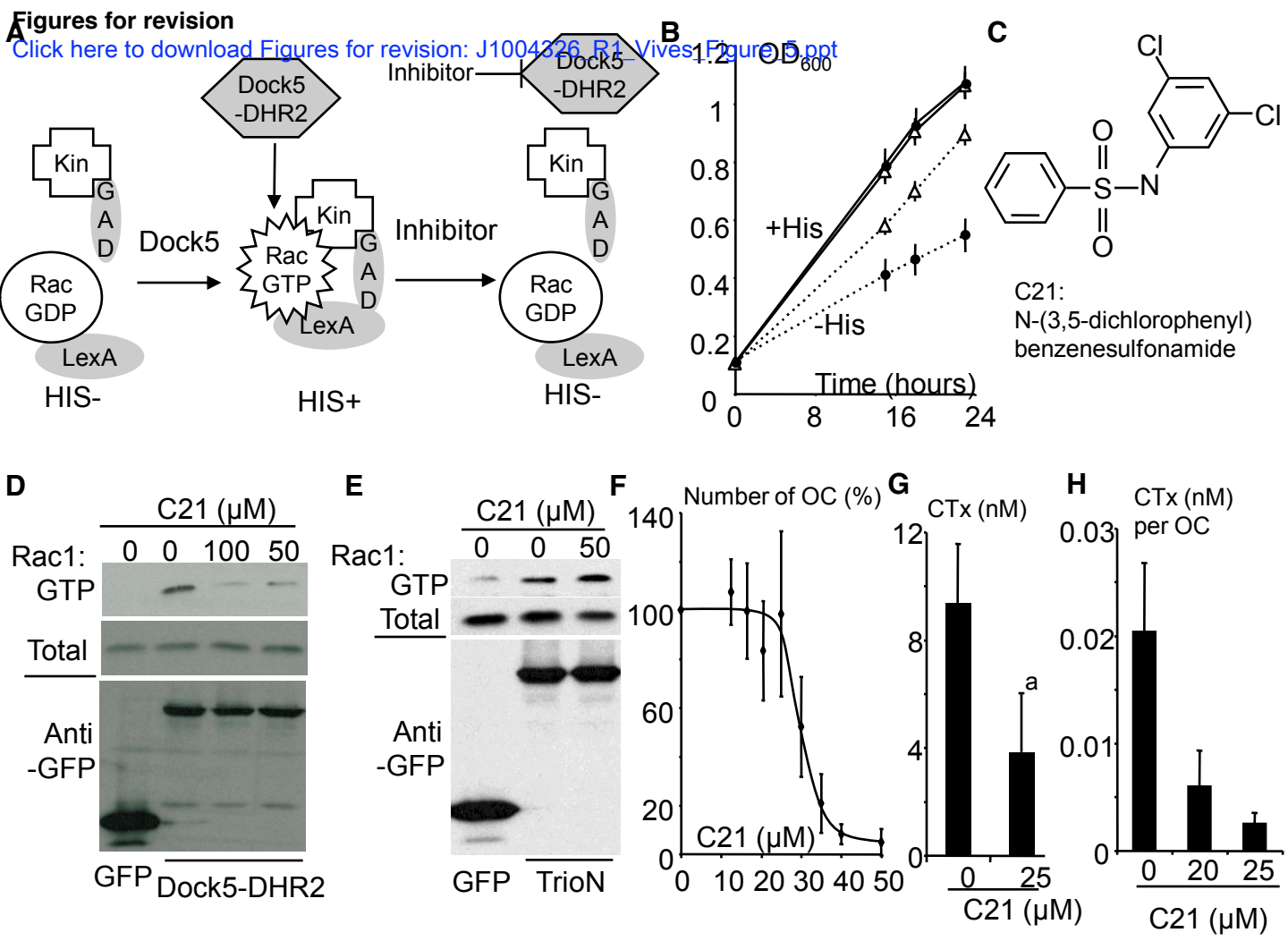

Vives et al., Figure 5

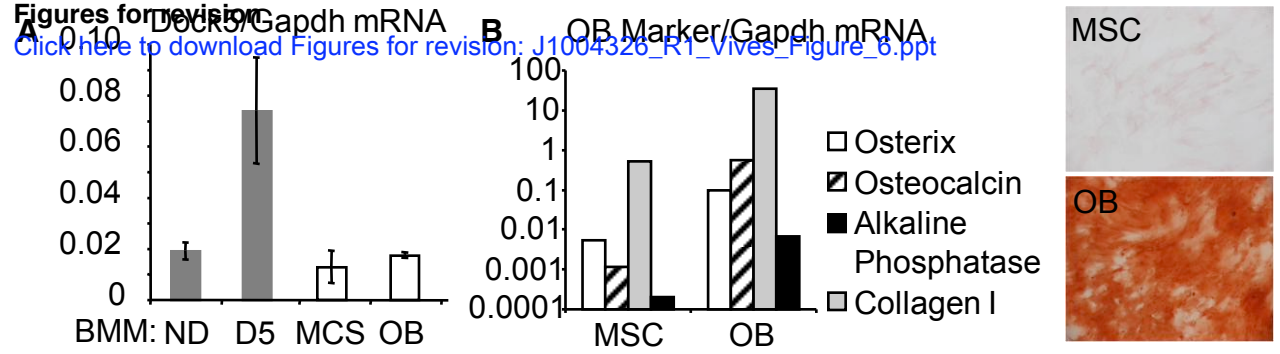

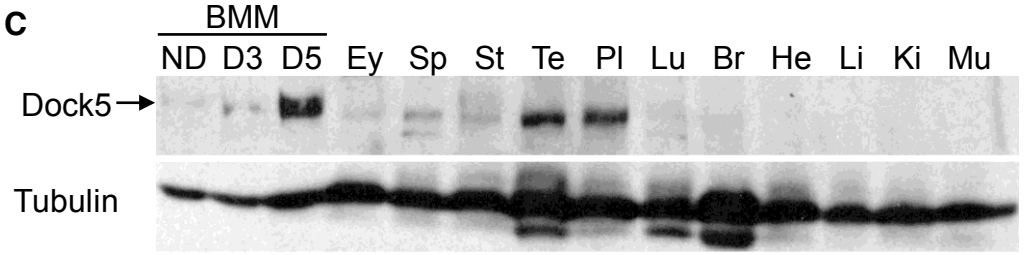

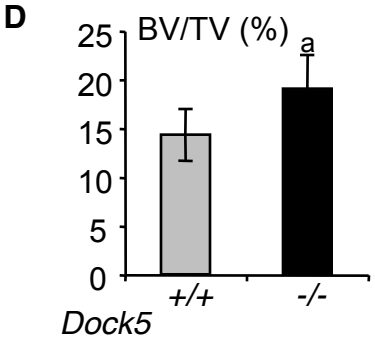

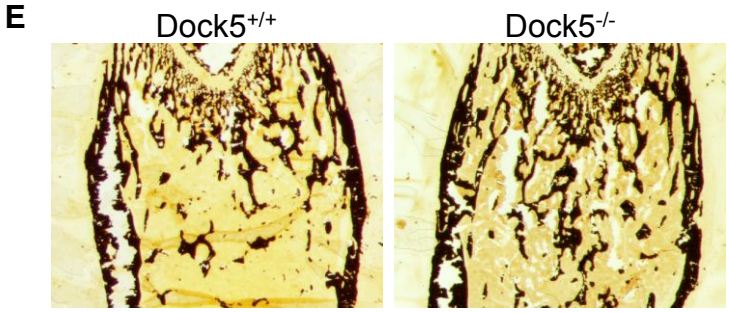

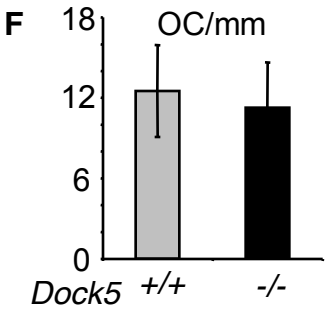

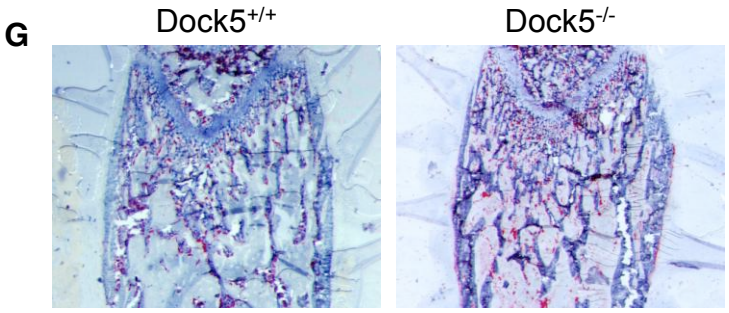

Vives et al., Figure 6

Figures for revision

Click here to download Figures for revision: J1004326_R1_Vives_Figure_7.ppt

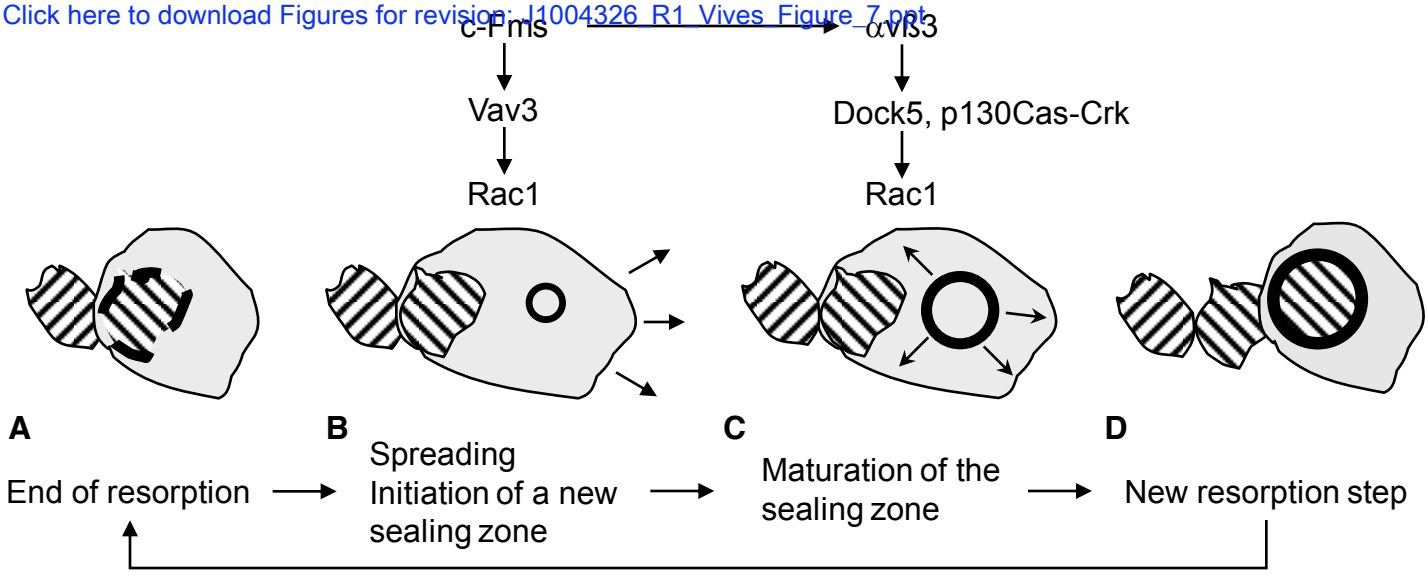

Vives et al., Figure 7

Supplementary Information

Figure S1: Dock5 is essential for the formation of the sealing zone in osteoclasts.

(A) Western blot showing the expression of Dock5 and Gapdh in extracts from RAW264.7 cells expressing shRNAs against Luciferase (shLuc) or Dock5 (shDock5) at days 0, 3 and 5 of differentiation. **(B)** Osteoclasts differentiated from RAW264.7 cells expressing shLuc or shDock5 were fixed and stained to reveal the activity of Tartrate Resistant Acid Phosphatase (TRAP). Scale bars 200 μm **(C)** Osteoclasts differentiated on calcium-phosphate substrate were fixed and stained for actin to reveal the sealing zones (arrows). Scale bars 100 μm **(D)** Osteologic Biocoat matrices were stained with von Kossa to reveal resorbed areas (clear zones). Graph shows average and standard deviation (SD) resorbing activity per osteoclast obtained by measuring the resorbed area using ImageJ and dividing by the number of osteoclasts from two independent experiments performed in triplicates. **(E)** Osteoclasts differentiated from BMMs expressing shLuc or shDock5 on calcium-phosphate substrate substrate were fixed and stained for actin to reveal the sealing zones (arrows). Scale bars 100 μm **(F)** Average and SD CTx concentration per osteoclast in one experiment performed in triplicates and representative of three experiments.

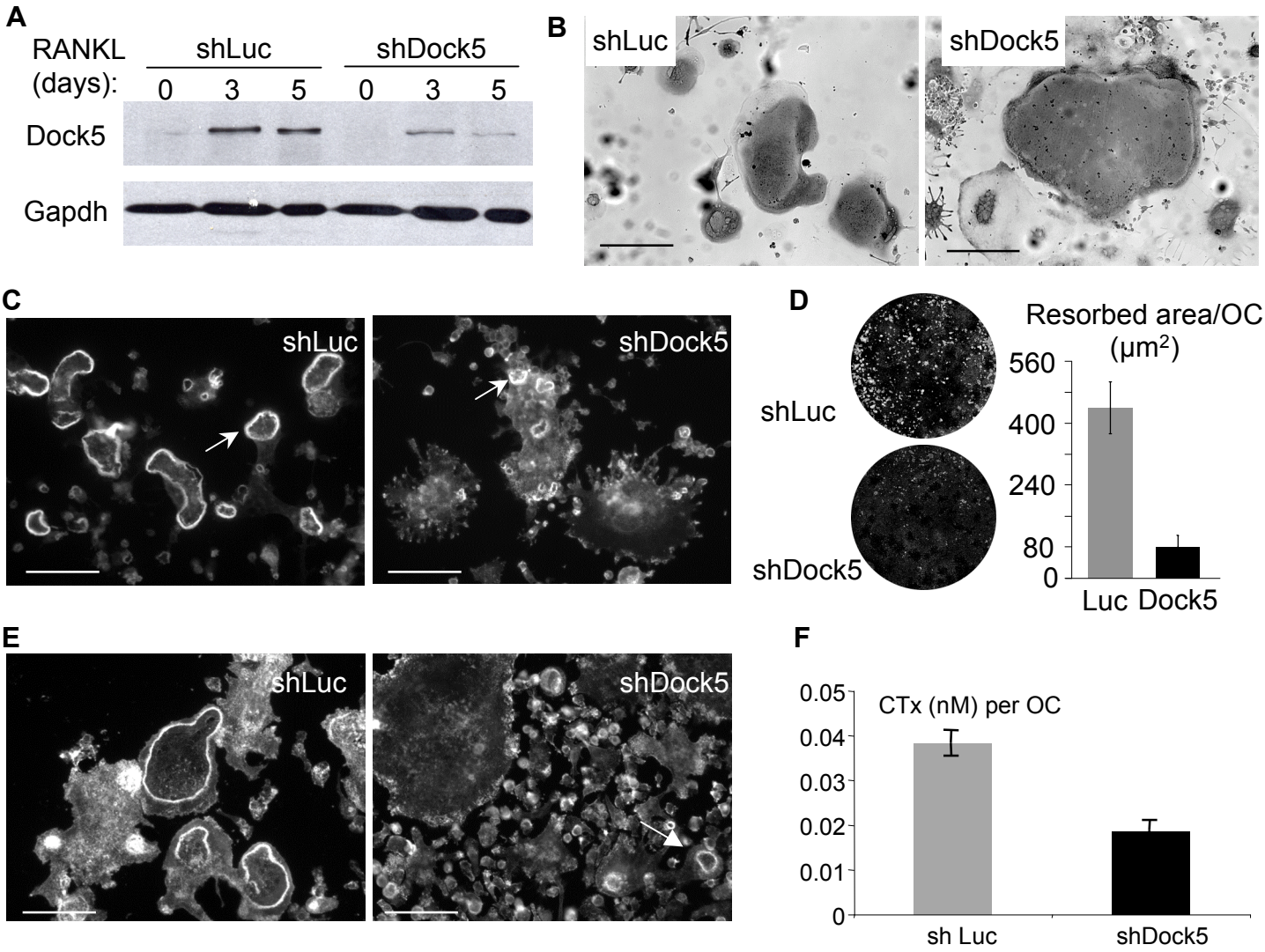

Vives et al., Figure S1